Tailorable Doping-Spike PtSi Infrared Detectors Fabricated by Si Molecular Beam Epitaxy

T. L. Lin, J. S. Park, S. D. Gunapala, E. W. Jones, and H. M. del Castillo

Center for Space Microelectronics Technology

Jet Propulsion Laboratory, California Institute of Technology

Pasadena, CA 91109

ABSTRACT

By incorporating a 1 -rim-thick p^+ doping spike at the PtSi/Si interface, we have successfully demonstrated extended cutoff wavelengths of PtSi Schottky infrared detectors. The extended cutoff wavelengths resulted from the reduced effective potential barriers due to the combined effects of an increased electric field near the silicide/Si interface and the Schottky image force. The p+ doping spikes were grown by molecular beam epitaxy at 450 "C using elemental boron as the dopant source, with doping concentrations ranging from 5 x 10^{19} to 2 x 10^{20} cm^{-3}. The cutoff wavelengths were shown to increase with increasing doping concentrations of the p+ spikes. Thermionic emission dark current characteristics were observed and photoresponse in the LWIR regime was demonstrated. Furthermore, the effective potential barriers determined by the Richardson plots were used to study the electrically activated boron dopant concentrations of the thin (1-rim-thick) spikes.

1. INTRODUCTION

The PtSi Schottky infrared (IR) detector one of the most promising IR detectors for large focal plane array (FPA) applications because it is Si-compatible, with advantages of easy integration with Si readout multiplexer to form large, uniform, and low-cost imaging arrays. Currently, PtSi provides the largest IR FPA's, with 640 x 480 and 1024 x 1024 element imaging arrays commercially available".

However, PtSi FPA's are limited for applications in the 1-3 and 3-5 μm regions due to the 5.5 μm cutoff wavelength determined by $\lambda_c = 1.24/q\phi_B$, where $q\phi_B = 0.22$ eV is the PtSi Schottky barrier on p-type Si. The spectral response of the PtSi IR detector follows the modified Fowler dependence, given by

$$\eta = C_1 \frac{(h\nu - q\phi_B)^2}{h\nu} = 1.24\ C_1 \lambda \left(\frac{1}{\lambda} - \frac{1}{\lambda_c}\right)^2 \qquad (1)$$

where η is the quantum efficiency (QE), C_1 is the emission coefficient, $h\nu$ and λ are the energy and the wavelength of the incident photon, respectively. Figure 1 shows the QE as a function of the wavelength calculated from Eq. 1 for various cutoff wavelength assuming $C_1 = 0.2$ eV^{-1}. The spectral response for a typical PtSi detector with λ_c = 5.5 μm decreases drastically with increasing wavelength, resulting in a relatively low response in the 3-5 μm medium wavelength infrared (MWIR) region. The spectral response can be greatly improved by extending the cutoff wavelength through the reduction of the effective Schottky barrier $q\phi_B$. As shown in Fig. 1, by extending the PtSi cutoff wavelength from 5.5 to 7 μm, more than one order of magnitude increase of the QE at 5 μm can be achieved. Furthermore, long wavelength infrared (LWIR) response can be obtained by extending the cutoff wavelength beyond 8 pm.

One approach to reduce the effective Schottky barrier is the incorporation of a doping spike at the silicide/Si interface. Due to the enhanced electrical field established by the charge of the depleted doping spike, a potential spike was formed near the silicide/Si interface, allowing carriers to tunnel into the substrate, resulting in a lower effective potential barrier. Previous approaches utilized relatively thick doping spikes (> 10 rim), formed by either ion implantation or molecular beam epitaxy (MBE)6-10. Very shallow ion implants at the metal-silicon interface, first demonstrated by Shannon[6], have been employed by Pellegrini *et a/.* and Wei *et a/.* to extend the PtSi cutoff wavelength[7,8]. More recently, molecular beam epitaxy (MBE) was used to grow the thin doping spikes to reduce the Schottky barriers of Ti/Si[9] and $CoSi_2$/Si[10]. However, the additional tunneling process required for the collection of the photo-excited carriers due to the presence of the potential spike reduces the detector response.

The effective Schottky barrier can be reduced without the formation of the potential spike by reducing the spike thickness to less than 1 nm. This is due to the fact that the image-force effect is very strong within 1 nm from the silicide/Si interface. Figure 2 shows the calculated energy-band diagram of a PtSi detector with a 1 -nm-thick p^+ spike doped with 1.2 x 10^{20} cm^{-3} boron. The substrate doping concentration is 5 x 10^{14} cm^{-3}, and the bias voltage is -1 V The effective barrier is reduced to 0.1 eV, corresponding to a cutoff wavelength of 12.4 µm without a potential spike, and consequently, no tunneling process will be involved in the internal photo emission process.

The use of thin doping spikes required a significant increase of the spike doping concentration. The barrier reduction $\Delta q\phi$ is given approximately by

$$\Delta q\phi = \frac{q}{\varepsilon_S} N d^2 \qquad (2)$$

where N and d are the doping concentration and the thickness of the doping spike, respectively. Consequently, an increase of the doping concentration by two orders of magnitude is required for the I-rim-thick doping spikes compared to previous 10-nm-thick spikes. This can be accomplished using Si MBE growth technology [1]112. Eq. 2 can also be used to study the electrically activated boron doping concentration of thin (1-rim-thick) doping spikes.

II. MBE GROWTH AND DETECTOR FABRICATION

The PtSi Schottky detectors were fabricated on double-side polished Si (1 00) wafers with a resistivity of 30 Q-cm. The device structure incorporates n-type guard rings which define the periphery of the active device areas to suppress edge leakage. Prior to MBE growth, the wafers were cleaned using the "spin-clean" method, which involves the removal of a chemically grown surface oxide using an HF/ethanol solution in a nitrogen glove box followed by annealing in the growth chamber of a commercial Riber EVA 32 Si MBE system at temperatures less than 500°C[13]. The 1 -rim-thick p^+-Si layers were grown by MBE at 450 "C using elemental boron as the dopant source. The iow growth temperature is essential to preserve the atomically sharp doping profiles to avoid the boron precipitation and surface segregation problems[11]. Doping concentrations ranging from 5 x 10^{19} to 2 x 10^{20} cm^{-3} were studied. The 4-rim-thick PtSi layers were formed in-situ by depositing 2-rim-thick Si followed by 2-rim-thick Pt, and then annealing at 400°C for 20 min. The schematic cross section of the doping-spike PtSi detector was shown in Fig. 3. The devices were characterized using current-voltage (I-V) measurements and photoresponse measurements.

III. RESULTS AND DISCUSSION

The dark currents of the doping-spike PtSi detectors were thermionic emission limited, given by

$$J_o = A^{**} T^2 e^{-q\phi_B/kT}, \qquad (3)$$

where Jo is the dark current density, A** is the Richardson constant, T is the absolute temperature, $q\phi_B$ is the effective potential barrier, and k is the Boltzmann constant. The current-voltage (I-V) characteristics of a typical doping spike PtSi detector is shown in Fig. 4. The doping concentration of the I-rim-thick p^+ doping spike is 2 x

10^{20} cm^{-3}. The effective barrier height can be obtained from the Richardson plot by linealizing Eq. (3)

$$\ln\left(\frac{J_0}{T^2}\right) = -\frac{q\phi_B}{kT} + \ln(A^{**}). \qquad (4)$$

Figure 5 shows the Richardson plot atypical doping-spike PtSi detector at -0.5 V bias. Thermionic-emission limited characteristics were observed at temperatures ranging from 22 to 46 K, with a five orders of magnitude current density range. An effective barrier height $q\phi_B$ of 0.032 eV was determined from the slope of the plot, compared to 0.206 eV of PtSi detectors without a doping spike. From Eq. 2, the electrically activated boron doping concentration N is given by

$$N = \frac{2\,\varepsilon_s\,\Delta q\phi}{q\,d^2}. \qquad (5)$$

The effective barriers and the calculated electrically activated boron doping concentrations for three doping-spike PtSi detectors are shown in Table 1. As shown in Table 1, the effective barrier can be tailored by varying the doping concentration of the doping spike, and electrically activated boron doping concentrations ranging from 8.7 x 10^{18} cm-3 to 2.3 x 10^{20} cm-3 have been achieved in the 1 -rim-thick spikes.

The detector spectral responses were measured with back-side illumination using a 940K blackbody source. Figure 6 shows the responses of three doping-spike PtSi detectors. Also shown in Fig. 6 is the calculated response of a conventional PtSi detector with C_1 = 0.2 eV^{-1} and λ_c = 5.5 μm for comparison. For the doping-spike PtSi detectors, a significantly increased MWIR response was observed. For example, an QE increase by 30 times was achieved at 5 μm, compared to the conventional PtSi detector. In the LWIR regime, the detector response increased with increasing cutoff wavelength, as expected by the Fowler dependence. The response of the 14 μm cutoff detector in the 8-12 μm region is similar to that of the conventional PtSi detector in the 4-5 μm region, providing a useful response for LWIR applications. At 12 μm, the

QE is increased by factors of 4.4 and 7.6 by extending the cutoff wavelength to 18 and 22 µm, respectively.

IV. SUMMARY

In conclusion, the cutoff wavelength of the PtSi Schottky nfrared detector has been extended to the LWIR region by incorporating a 1-nm-thic (p+ doping spike at the silicide/silicon interface. The use of the 1 -rim-thick doping spike eliminated the formation of the potential spike of the previous approaches, resulting in an improved detector response. Thermionic emission I-V characteristics and Fowler-dependent photoresponses were observed for the doping-spike PtSi detectors, indicating the absence of undesirable tunneling mechanism. Electrically activated boron doping concentrations of the 1 -rim-thick spikes were determined from the reduction of the barrier heights. Tailorable cutoff wavelengths of 14, 18, and 22 µm have been demonstrated by varying the doping concentrations of the p+ spikes.

v. ACKNOWLEDGMENT

The work described in this report was performed by the Center for Space Microelectronics Technology, Jet Propulsion Laboratory, California Institute of Technology and was jointly sponsored by the National Aeronautics and Space Administration/Office of Advanced Concepts and Technology, the Ballistic Missile Defense Organization/Innovative Science and Technology Office, and the Air Force Rome Laboratory.

REFERENCES

1. D. J. Sauer, F. V. Shallcross, F. L. Hsueh, G. M. Meray, P. A, Levine, H. R. Gilmartin, T. S, Villani, B. J. Esposito, and J. R. Tower, Proc. SPIE, Vol. 1540, *Infrared Technology XV//,* edited by B. F. Andresen, M. Scholl, and 1. J. Spiro, pp. 285-296 (SPIE, Bellingham, 1991).
2. J. L. Gates, W. G, Connelly, T. D. Franklin, R. E. Mills, F. W. Price, and T. Y. Wittwer, Proc. SPIE, Vol. 1540, *Infrared Technology XV//,* edited by B. F. Andresen, M. Scholl, and 1. J. Spiro, pp. *297-302,* (SPIE, Bellingham, 1991).
3. D. L. Clark, J. R. Berry, G. L. Compagna, M. A, Cosgrove, G. G. Furman, J. R, Heydweiller, H. Honickman, R. A. Rehberg, P. H. Solie, and E. T. Nelson, Proc. SPIE, Vol. 1540, *Infrared Technology XV//,* edited by B. F. Andresen, M. Scholl, and 1. J. Spiro, pp. 303-311, (SPIE, Bellingham, 1991).
4. M. Kimata, N. Yutani, and S. N. Tsubouchi, Proc. SPIE. Vol. 1762, *Infrared Technology XV///,* edited by B. F. Andresen and F. D. Shepererd (SPIE, Bellingham, 1991) (to be published).
5. S. M. Sze, *Physics of Semiconductor Devices* (Wiley, New York, 1981), Chap. 5.
6. J. M. Shannon, Appl. Phys. Lett., 24, 369 (1974).
7. P. Pellegrini, M. Week, and C. E. Ludington, Proc. SPIE, Vol. 311, *Mosaic focal Plane Methodologies //,* edited by W. S. Chan and J. T. Hall, pp. 24-29 (SPIE, Bellingham, 1981).
8. C-Y. Wei, W, Tantraporn, W Katz, and G. Smith, Thin Solid Films, 93, 407, 1982.
9. W. C. Ballamy and Y. Ota, Appl. Phys, Lett., 39 629 (1981).
10. R. W. Fathauer, T. L. Lin, P. J. Grunthaner, J Maserjian, and P. O. Andersson, Proc. SPIE, Vol. 877, *Innovative Science and Technology,* edited by C. Kukkonen, pp. 2-7, (SPIE, Bellingham, 1988)
11. C. P. Parry, S. M. Newstead, R. D. Barlow, P. Augustus, R. A. A. Kubiak, M.G, Dowsett, T. E. Whall, and E. H. c. Parker, Appl. Phys, Lett., 58, 181 (1991).

12. T. L. Lin, T. George, E. W. Jones, and A. Ksendzov, Appl. Phys. Lett., 60, 380 (1992).

13. P. J. Grunthaner, F. J. Grunthaner, R. W. Fathauer, T. L. Lin, F. D. Schowengerdt, M. H. Hecht, D. Bell, W. Kaiser, and J. H. Mazur, Thin Solid Films, 183, 197 (1989).

TABLE 1. The effective barrier heights and the calculated electrically activated boron doping concentrations of the spikes for the doping-spike PtSi detectors.

Sample	effective barrier height eV	calculated electrically activated [B] cm-3
PtSi	0.206	
A	0.186	8.7×10^{18}
B	0.054	2.0×10^{20}
c	0.032	2.3×10^{20}

FIGURE CAPTION

Figure 1. The calculated quantum efficiency of PtSi Schottky infrared detectors with various cutoff wavelength.

Figure 2. The calculated energy-band diagram of the doping-spike PtSi detector incorporating the Schottky image force effect. The spike is 1 nm thick and doped with 1.2 x 10^{20} cm^{-3} boron.

Figure 3. The schematic cross section of the doping-spike PtSi detector.

Figure 4. The reverse current-voltage characteristics of a typical doping-spike PtSi detector at temperatures ranging from 22 to 46 K. The active device area is 6 x 10-4 cm2.

Figure 5. Richardson plot of a typical doping-spike PtSi detector.

Figure 6. Quantum efficiency as a function of wavelength for the three doping-spike PtSi detectors with 1-rim-thick p+ doping spikes. The cutoff wavelengths can be tailored from 14 to 22 μm by increasing the doping concentration of the spike.

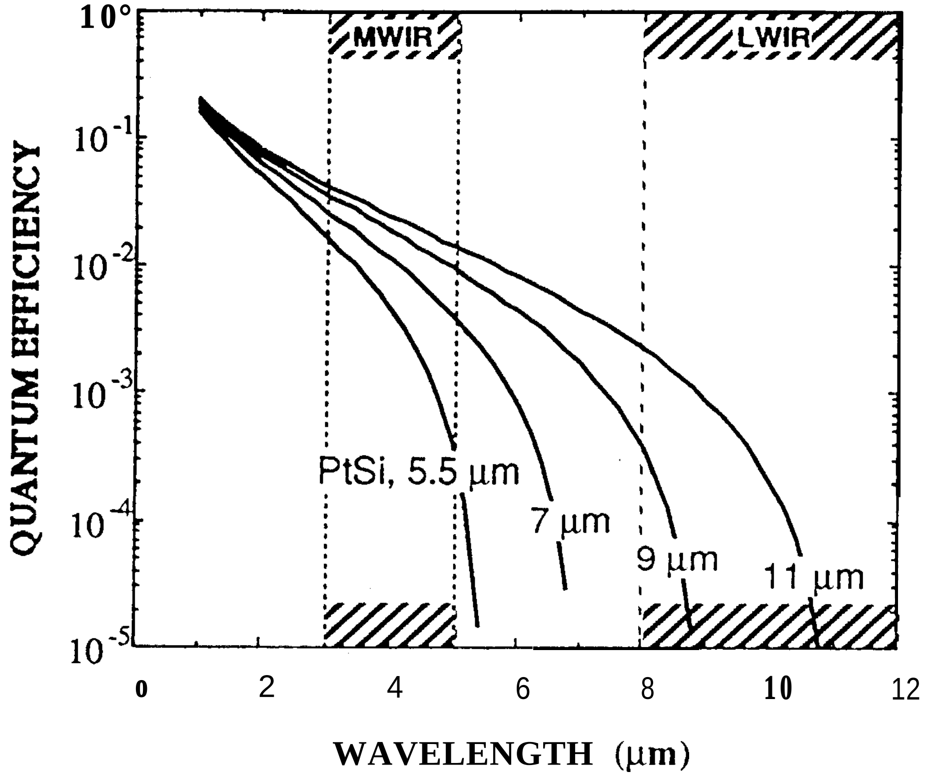

QUANTUM EFFICIENCY
10°
10-1
10-2
10-3
10-4
10-5
MWIR
LWIR
PtSi, 5.5 µm
7 µm
9 µm
11 µm
0
2
4
6
8
10
12
WAVELENGTH (µm)

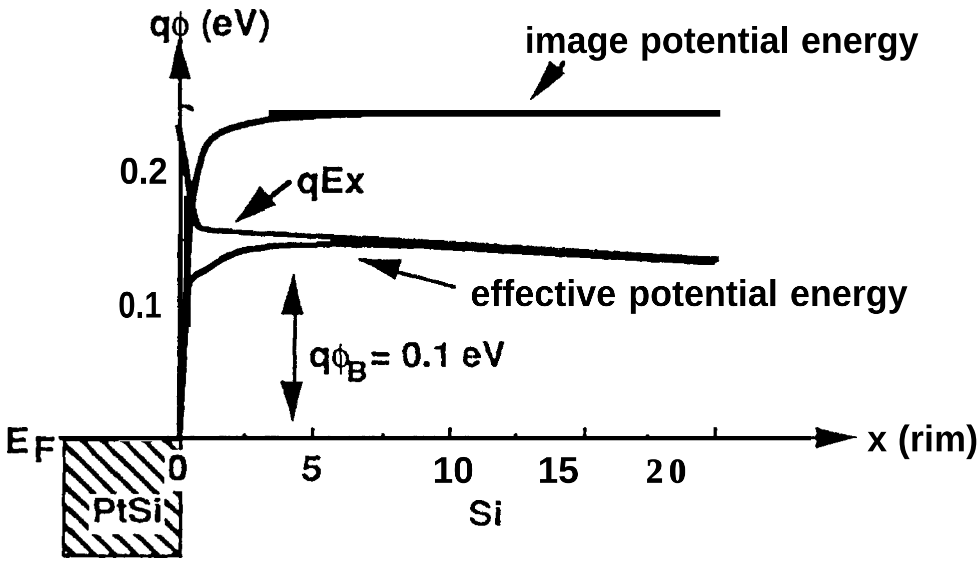

qϕ (eV)
image potential energy
0.2
qEx
0.1
effective potential energy
qϕB = 0.1 eV
EF
0
5
10
15
20
x (rim)
PtSi
Si

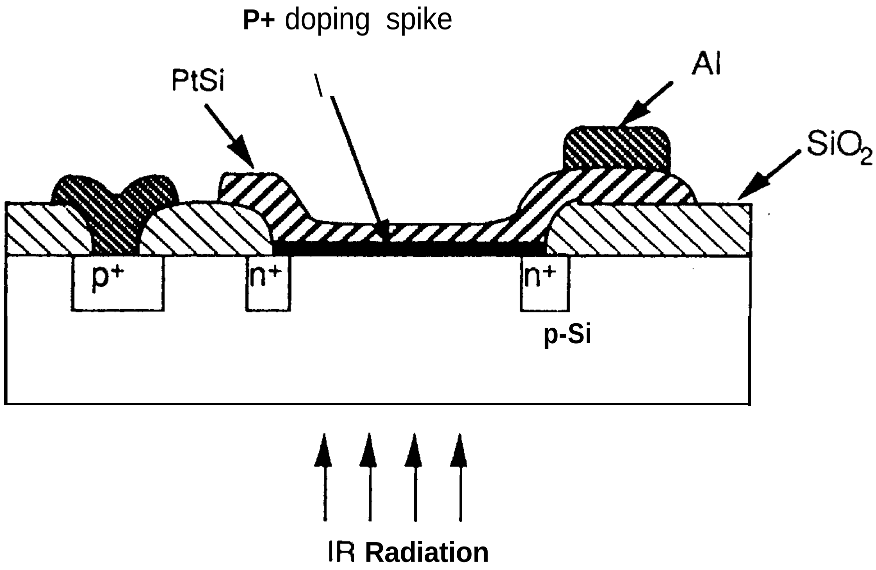
P+ doping spike
PtSi
Al
SiO2
p+
n+
n+
p-Si
IR Radiation

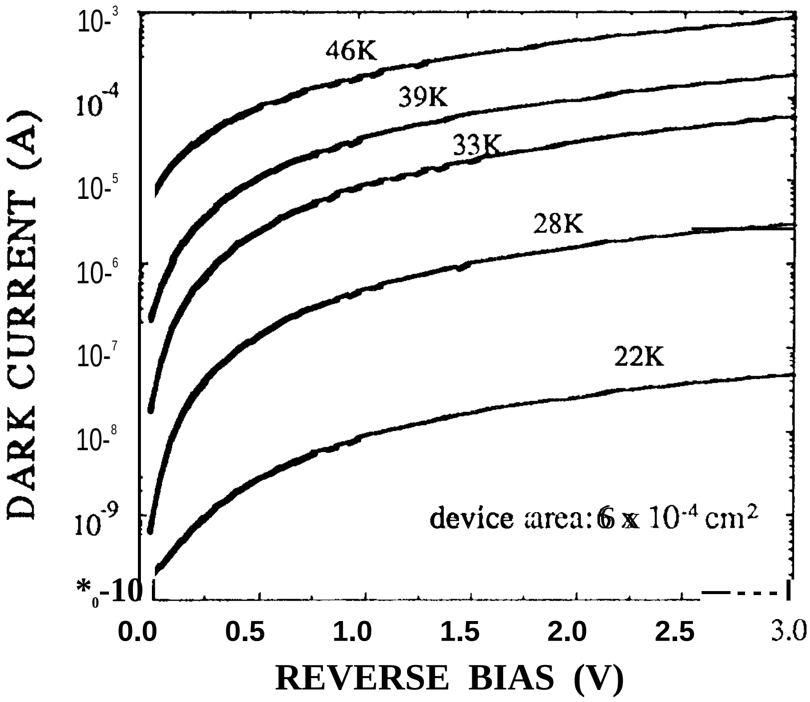

46K
39K
33K
28K
22K
device area: 6 x 10-4 cm2
DARK CURRENT (A)
REVERSE BIAS (V)
10-3
10-4
10-5
10-6
10-7
10-8
10-9
0.0
0.5
1.0
1.5
2.0
2.5
3.0

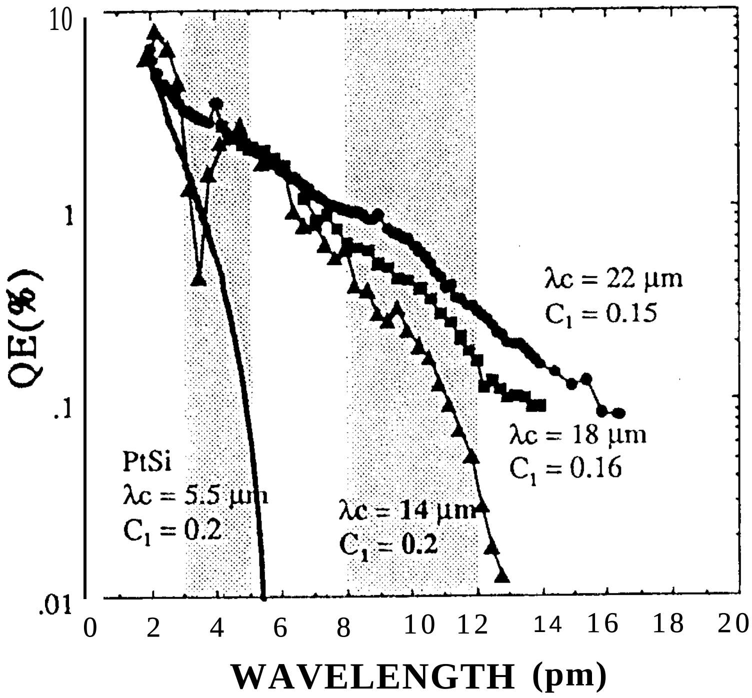

10
1
.1
.01
QE(%)
0
2
4
6
8
10
12
14
16
18
20
WAVELENGTH (pm)
λc = 22 µm
C1 = 0.15
λc = 18 µm
C1 = 0.16
λc = 14 µm
C1 = 0.2
PtSi
λc = 5.5 µm
C1 = 0.2